

Anisotropic ferro- and piezoelectric properties of sol-gel-grown $\text{Bi}_{3.15}\text{Nd}_{0.85}\text{Ti}_3\text{O}_{12}$ films with two different orientations on Pt/Ti/SiO₂/Si

C. J. Lu^{a)}

Department of Materials Science and Engineering, Hubei University, Wuhan 430062,
People's Republic of China and Max Planck Institute of Microstructure Physics, Weinberg 2,
D-06120 Halle, Germany

X. L. Liu, X. Q. Chen, and C. J. Nie

Department of Materials Science and Engineering, Hubei University, Wuhan 430062,
People's Republic of China

Gwenael Le Rhun, Stephan Senz, and Dietrich Hesse

Max Planck Institute of Microstructure Physics, Weinberg 2, D-06120 Halle, Germany

(Received 20 March 2006; accepted 18 June 2006; published online 7 August 2006)

$\text{Bi}_{3.15}\text{Nd}_{0.85}\text{Ti}_3\text{O}_{12}$ thin films of two different preferred orientations were sol-gel grown on Pt/Ti/SiO₂/Si. Using different heating rates during crystallization, either films containing 65% columnar grains with (104)/(014) orientation or fine-grained films with a predominant *c*-axis orientation were obtained. Anisotropic ferroelectric and piezoelectric properties were determined, with a remanent polarization $2P_r=46.4 \mu\text{C}/\text{cm}^2$ and a piezoelectric coefficient $d_{33}=17 \text{ pm}/\text{V}$ in a predominantly (104)/(014)-oriented film, but only $2P_r=16.7 \mu\text{C}/\text{cm}^2$ and $d_{33}=5 \text{ pm}/\text{V}$ in a predominantly *c*-axis-oriented film. These values confirm that the polarization vector of this material is close to the crystallographic *a* axis. © 2006 American Institute of Physics.

[DOI: 10.1063/1.2335409]

Ferroelectric thin films have been widely investigated in view of their applications in nonvolatile memories, piezoelectric microactuators, and resonators. Rare-earth element-substituted $\text{Bi}_4\text{Ti}_3\text{O}_{12}$ films are promising due to their fatigue endurance on Pt electrodes.^{1,2} $\text{Bi}_{3.15}\text{Nd}_{0.85}\text{Ti}_3\text{O}_{12}$ (BNdT) films have received attention for their large remanent polarization P_r .³⁻⁹ $\text{Bi}_4\text{Ti}_3\text{O}_{12}$ is monoclinic with the space group *B1a1* but can be considered pseudoorthorhombic with $a=0.545 \text{ nm}$, $b=0.541 \text{ nm}$, and $c=3.283 \text{ nm}$. For nonsubstituted $\text{Bi}_4\text{Ti}_3\text{O}_{12}$ single crystals, the major component of spontaneous polarization (P_s) lies along the *a* axis ($\approx 50 \mu\text{C}/\text{cm}^2$); the component along the *c* axis is very small ($\approx 4 \mu\text{C}/\text{cm}^2$).¹⁰ This ferroelectric anisotropy requires the growth of *non-c-axis-oriented* films to achieve large P_r values in planar-type capacitors. For BNdT, the data of some authors^{4,5,7,11} point to a similar ferroelectric anisotropy as for $\text{Bi}_4\text{Ti}_3\text{O}_{12}$, whereas other authors⁹ obtained contradicting results. If the major polarization component of BNdT is along the *a* axis, films having a larger fraction of *non-c-axis-oriented* grains should exhibit better ferro- and piezoelectric properties. However, such films tend to grow with the *c* axis perpendicular to the film plane on standard-type Pt/Ti/SiO₂/Si substrates.

Recently, the growth of rare-earth element-substituted $\text{Bi}_4\text{Ti}_3\text{O}_{12}$ films with *a*-axis or *a/b*-axis orientation^{3,4,12-14} and with (104)/(014) orientation^{5,8,15,16} on conducting oxide layers was reported, and all this work confirmed the crucial role of the crystallographic orientation. Unfortunately, there are very few reports on such oriented films grown directly on noble metal electrodes^{7,17,18} or on SrRuO₃-buffered metal electrodes.^{8,19} We previously reported on a route to grow

BNdT films with predominant *a/b*-axis orientation on (111)Pt/Ti/SiO₂/Si through a sol-gel process and on the large anisotropy of their ferroelectric and dielectric properties.⁷ The present letter reports on BNdT films directly grown on (111)Pt/Ti/SiO₂/Si with predominant (104)/(014) orientation, quantifies the amount of the predominant orientation, considers their microstructure, and compares their properties with those of predominantly *c*-axis-oriented films.

The BNdT thin films were deposited on (111)Pt/Ti/SiO₂/(100)Si using a sol-gel process. Appropriate amounts of $\text{Bi}(\text{NO}_3)_3 \cdot 5\text{H}_2\text{O}$, $\text{Nd}(\text{CH}_3\text{COO})_3$, and $\text{Ti}(\text{OC}_4\text{H}_9)_4$ were dissolved in an acidic solution. 4 mol % excess bismuth nitrate was added to compensate for the Bi loss during annealing. The as-deposited films were pyrolyzed at 450 °C in air, followed by annealing at 750 °C in flowing oxygen. The deposition-crystallization cycles were repeated several times to obtain the desired thickness. The different crystallographic orientations [predominantly (104)/(014) and *c* axis] of the BNdT thin films were controlled by different heating rates during crystallization. A heating rate of 40 °C/min was used in the case of BNdT films with predominant (104)/(014) orientation whereas it was 10 °C/min for the predominately *c*-axis-oriented films. Pt top electrodes of typically 0.24 mm² in size were deposited by sputtering using a shadow mask. Details on the used methods of x-ray diffraction (XRD), transmission electron microscopy (TEM), piezoresponse force microscopy^{11,20} (PFM) and ferroelectric characterization (performed at a frequency of 1 kHz) are available elsewhere.^{3,6,8,16}

Figure 1 shows θ - 2θ scans and pole figures (insets, recorded with the BNdT 117 reflection) of two films with different preferred orientations. Both XRD patterns are indexed according to the standard powder diffraction data of

^{a)} Author to whom correspondence should be addressed; electronic mail: lcj@hubu.edu.cn

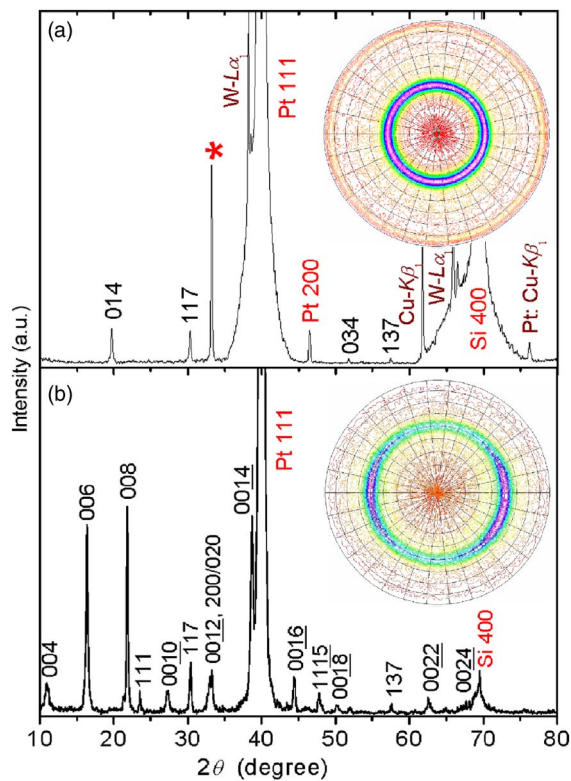


FIG. 1. (Color online) X-ray θ - 2θ diffraction patterns of BNdT thin films with (a) predominant (104)/(014) orientation (65%) and (b) predominant (001) orientation (50%). The peaks at $2\theta=38.22^\circ$, 61.74° , and 66.04° in (a) correspond to Pt W $L\alpha_1$, Si Cu $K\beta_1$, and Si W $L\alpha_1$, respectively. The sharp peak denoted with an asterisk in Fig. 1(a), located at the position of the forbidden Si (200) peak at $2\theta=33.08^\circ$, is in fact the Si(400) peak originating from half the Cu $K\alpha$ wavelength unintentionally passing the monochromator. The insets are x-ray pole figures recorded from the BNdT (117) reflection; the rim of the patterns corresponds to $\psi=90^\circ$.

$\text{Bi}_{3.6}\text{Nd}_{0.4}\text{Ti}_3\text{O}_{12}$.²¹ In the standard data, the 117 reflection is the strongest peak, and its intensity is about 100 times that of 014. In Fig. 1(a), the 014 peak is slightly stronger than the 117 peak, suggesting that the film is predominantly 104/014 oriented. The 104 reflection is prohibited due to systematic absences, see Ref. 5. The two rings at $\psi \approx 36^\circ$ and 84° in the pole figure of Fig. 1(a) correspond to the (117)/(1 $\bar{1}$ 7) and (11 $\bar{7}$)/(1 $\bar{1}$ 7) reflections, respectively. Because of the angles $\angle(104):(117)=36.4^\circ$ and $\angle(104):(11\bar{7})=84.1^\circ$, the pole figure confirms the predominant (104)/(014) orientation of the film, with a random in-plane orientation. The background intensities are in the range of 20–80 counts/s, while the maximum intensity at the ring $\psi \approx 36^\circ$ is about 790 counts/s, indicating a mixture of (104)/(014) and random orientations. According to the x-ray pole figure, the volume fraction of the (104)/(014)-oriented grains in the film can be estimated to be around 65%.

In the XRD pattern of Fig. 1(b), very strong (00 l) reflections are present besides other peaks, suggesting that the BNdT film is predominantly c axis oriented. The pole figure showing a ring at $\psi \approx 51^\circ$ confirms this, cf. $\angle(001):(117)=50.8^\circ$. The intensity distribution along the ring points to some preferential azimuthal orientation of the (001)-oriented grains. The background intensity of the pole figure ranges from 20 to 70 counts/s, while the maximum intensity of the ring at $\psi \approx 51^\circ$ is about 340 counts/s. This indicates that the BNdT film is a mixture of c -axis and random orientations.

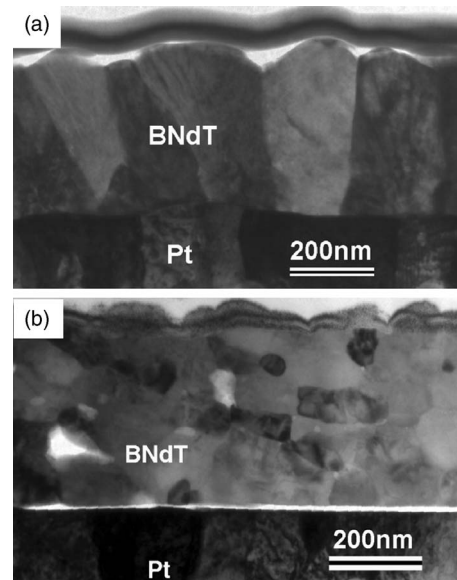


FIG. 2. Cross-sectional TEM images of the BNdT films (a) with predominant (104)/(014) orientation and (b) with predominant (001) orientation. The gap between the film and the bottom Pt electrode in (b) was formed during TEM specimen preparation.

The volume fraction of the c -axis-oriented grains was estimated to be around 50%.

Figure 2 shows cross-sectional TEM images of the two films. The film with predominant (104)/(014) orientation consists of large columnar grains. High-resolution TEM investigations (not shown) revealed that the (104)/(014)-oriented columnar grains generally nucleate on the Pt bottom electrode. In contrast, the predominantly c -axis-oriented film consists of equiaxed fine grains of 50–150 nm in diameter, as shown in Fig. 2(b). High resolution TEM observations (not shown) indicate that the c -axis-oriented grains are almost randomly located in the film. Detailed TEM observations are in agreement with the XRD results regarding the preferred orientations of the two films. The different microstructures of the two films can be understood in terms of the faster growth rate of BNdT grains along the a/b axes than along the c axis, and if the latter have a higher nucleation density than the former. The anisotropic growth of layered perovskites such as $\text{Bi}_4\text{Ti}_3\text{O}_{12}$ is well known.¹⁰

The formation of a predominant (001) orientation is thought to be driven by its low surface energy, i.e., by thermodynamics. As a consequence, Bi-layered films of this kind prefer to grow c axis oriented, when the growth conditions (e.g., high growth temperatures, slow heating rates, low deposition rates) permit this. However, if non- c -axis-oriented growth is aimed at, kinetic growth conditions (e.g., high deposition rates or rapid temperature ramping) are required, as observed for (100)-oriented $\text{YBa}_2\text{Cu}_3\text{O}_{7-\delta}$ (Ref. 22–24) and $(\text{Bi}, \text{La})_4\text{Ti}_3\text{O}_{12}$ films.³ Indeed we found that heating rapidly for crystallization is crucial for the growth of our (104)/(014)-oriented films, which points to a kinetic growth regime in this case.

Figure 3 shows the polarization-electric field (P - E) hysteresis loops of the corresponding film capacitors. Both films have an identical coercive field E_c of ~ 140 kV/cm, higher than that of (104)/(014)-oriented BNdT epitaxial films ($E_c = 50$ kV/cm) but lower than that of a/b -axis-oriented

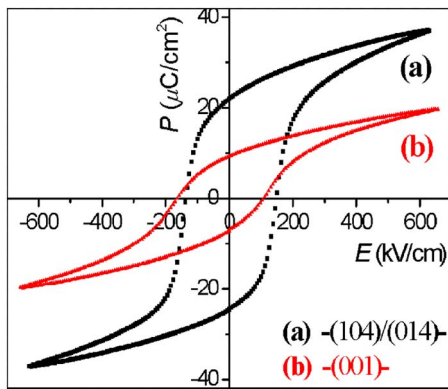


FIG. 3. (Color online) P - E hysteresis loops of the film capacitors (a) with predominant (104)/(014) orientation and (b) with predominant (001) orientation.

(Bi,La)₄Ti₃O₁₂ epitaxial films ($E_c=265$ kV/cm).^{3,5} The predominantly (104)/(014)-oriented film showed a $2P_r$ of ~ 46.4 $\mu\text{C}/\text{cm}^2$ at an applied voltage of 25 V, whereas the predominantly c -axis-oriented film showed $2P_r \approx 16.7$ $\mu\text{C}/\text{cm}^2$. Considering the possible difficulty of 90° domain switching in BNdT,⁴ the remanent polarization of the predominantly (104)/(014)-oriented film is the sum of two parts from (104)-oriented grains and from randomly oriented grains in the film, while the contribution of the (014)-oriented grains should be negligible. Interestingly, the $2P_r$ of 46.4 $\mu\text{C}/\text{cm}^2$ of our films is larger than the value reported for epitaxial (104)/(014)-oriented BNdT films ($2p_r = 40$ $\mu\text{C}/\text{cm}^2$).⁵

Figure 4 shows piezoelectric hysteresis loops—recorded by PFM—of the BNdT films with different preferred orientations. The effective remanent piezoelectric coefficient d_{33} of the predominantly c -axis-oriented film is about 5 pm/V at an applied field of 210 kV/cm, whereas a considerably higher value of 17 pm/V is obtained for the film with predominant (104)/(014) orientation. These results are in qualitative agreement with those measured from Bi₄Ti₃O₁₂ thin films by Harnagea *et al.*¹¹ Overall, the obtained results dem-

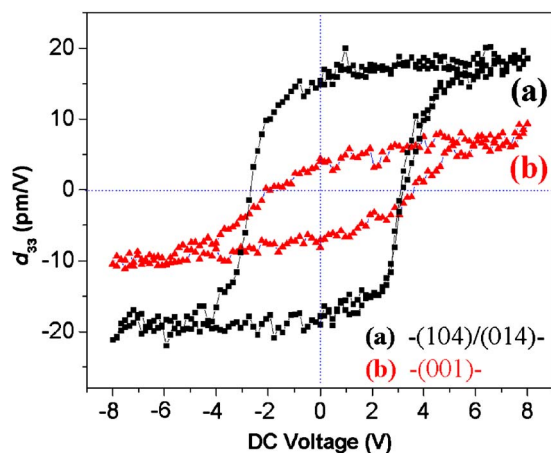


FIG. 4. (Color online) Piezoelectric hysteresis loops of the film capacitors corresponding to those in Fig. 3.

onstrate that the major component of the polarization in BNdT is parallel to the a axis.

In summary, ferroelectric BNdT thin films with predominant (104)/(014) orientation and with predominant c -axis orientation were deposited directly on Pt/Ti/SiO₂/Si substrates by a sol-gel process. Heating rapidly for crystallization is crucial for the nucleation of (104)/(014) oriented grains on Pt-coated Si. The $2P_r$ and d_{33} values of the BNdT films increase with the film orientation further away from the c axis. The anisotropic ferroelectric and piezoelectric properties support those findings that the major polarization direction in BNdT lies along the a axis.

The authors thank M. Alexe for helpful discussions and I. Vrejoiu for valuable technical assistance. This work was supported by the National Science Foundation of China (10474019), the Program for New Century Excellent Talents (NCET) in University, and the Science Foundation of Education Bureau of Hubei Province, China; work at MPI Halle was supported by DFG via SFB 418 and FOR 404.

¹C. A. P. de Araujo, J. D. Cuchiaro, L. D. McMillan, M. C. Scott, and J. F. Scott, *Nature (London)* **374**, 627 (1995).

²B. H. Park, B. S. Kang, S. D. Bu, T. W. Noh, J. Lee, and W. Jo, *Nature (London)* **401**, 682 (1999).

³H. N. Lee, D. Hesse, N. Zakharov, and U. Gösele, *Science* **296**, 2006 (2002).

⁴T. Watanabe, T. Kojima, H. Uchida, I. Okada, and H. Funakubo, *Jpn. J. Appl. Phys., Part 2* **43**, L309 (2004).

⁵A. Garg, Z. H. Barber, M. Dawber, J. F. Scott, A. Snedden, and P. Lightfoot, *Appl. Phys. Lett.* **83**, 2414 (2003).

⁶J. H. Li, Y. Qiao, X. L. Liu, C. J. Nie, C. J. Lu, Z. X. Xu, S. M. Wang, N. X. Zhang, D. Xie, H. C. Yu, and J. Q. Li, *Appl. Phys. Lett.* **85**, 3193 (2004).

⁷C. J. Lu, Y. Qiao, Y. J. Qi, X. Q. Chen, and J. S. Zhu, *Appl. Phys. Lett.* **87**, 222901 (2005).

⁸S. K. Lee, D. Hesse, and U. Gösele, *Appl. Phys. Lett.* **88**, 062909 (2006).

⁹U. Chon, H. M. Jang, M. G. Kim, and C. H. Chang, *Phys. Rev. Lett.* **89**, 087601 (2002).

¹⁰S. E. Cummins and L. E. Cross, *J. Appl. Phys.* **39**, 2268 (1968).

¹¹C. Harnagea, A. Pignolet, M. Alexe, D. Hesse, and U. Gösele, *Appl. Phys. A: Mater. Sci. Process.* **70**, 261 (2000).

¹²H. Matsuda, S. Ito, and T. Iijima, *Appl. Phys. Lett.* **85**, 1220 (2004).

¹³T. Watanabe, H. Funakubo, K. Saito, T. Suzuki, M. Fujimoto, M. Osada, Y. Noguchi, and M. Miyayama, *Appl. Phys. Lett.* **81**, 1660 (2002).

¹⁴T. Watanabe and H. Funakubo, *Jpn. J. Appl. Phys., Part 1* **44**, 1337 (2005).

¹⁵T. Kojima, T. Sakai, T. Watanabe, H. Funakubo, K. Saito, and M. Osada, *Appl. Phys. Lett.* **80**, 2746 (2002).

¹⁶H. N. Lee and D. Hesse, *Appl. Phys. Lett.* **80**, 1040 (2002).

¹⁷R. Iijima, *Appl. Phys. Lett.* **79**, 2240 (2001).

¹⁸G. D. Hu, I. H. Wilson, J. B. Xu, W. Y. Cheung, S. P. Wong, and H. K. Wong, *Appl. Phys. Lett.* **74**, 1221 (1999).

¹⁹G. Asayama, J. Lettieri, M. A. Zurbuchen, Y. Jia, S. Trolier-McKinstry, D. G. Schlom, S. K. Streiffer, J. P. Maria, S. D. Bu, and C. B. Eom, *Appl. Phys. Lett.* **80**, 2371 (2002).

²⁰*Nanoscale Characterization of Ferroelectric Materials: Scanning Probe Microscopy Approach*, edited by M. Alexe and A. Gruverman (Springer, Berlin, 2004).

²¹H. McMurdie, M. Morris, E. Evans, B. Paretzkin, W. Wong-Ng, and C. Hubbard, *Powder Diffr.* **1**, 84 (1986).

²²J. Fujita, T. Yoshitake, A. Kamijo, T. Satoh, and H. Igarashi, *J. Appl. Phys.* **64**, 1292 (1988).

²³C. B. Eom, A. F. Marshall, S. S. Laderman, R. D. Jacowitz, and T. H. Geballe, *Science* **249**, 1549 (1990).

²⁴Q. Zhong, P. C. Chou, Q. L. Li, G. S. Taraldsen, and A. Ignatiev, *Physica C* **246**, 288 (1995).